Published by IOP Publishing for Sissa Medialab

Received: *November 30, 2025*
Accepted: *February 2, 2026*
Published: *April 10, 2026*

17TH Topical Seminar on Innovative Particle and Radiation Detectors
Siena, Italy
15–19 September 2025

Demonstration of a small-scale version of the MUonE experiment

M. Pesaresi[a] **on behalf of the MUonE collaboration**

[a] *Blackett Laboratory, Imperial College, London SW7 2AZ, U.K.*

E-mail: mark.pesaresi@imperial.ac.uk

Abstract: A small-scale realisation of the MUonE experiment was successfully operated at the CERN SPS M2 beamline to validate the detector technologies and data-acquisition concepts required for a precision measurement of the hadronic contribution to the running of $\alpha(t)$ via μ-e elastic scattering. The Phase 1 setup, comprising three tracking stations, an electromagnetic calorimeter, a muon filter, and a prototype beam momentum spectrometer, achieved stable 40 MHz operation with high tracking efficiency, sub-nanosecond synchronisation, and spatial resolutions consistent with design expectations. A high-intensity 160 GeV muon beam directed at carbon graphite targets was used to produce a large sample of μ-e elastic scattering events. A real-time selection algorithm capable of identifying events of interest online, delivered over 5×10^{11} events to disk. A first evaluation of detector performance under realistic beam conditions is now in progress.

Keywords: Data acquisition concepts; Particle identification methods; Particle tracking detectors; Trigger concepts and systems (hardware and software)

https://doi.org/10.1088/1748-0221/21/04/C04022

2026 JINST 21 C04022

Contents

2026 JINST 21 C04022

1 Introduction

MUonE is a proposed experiment at the CERN SPS to measure the hadronic contribution ($\Delta\alpha_{\text{had}}$) to the running of the electromagnetic coupling, $\alpha(t)$, in the spacelike region relevant for predictions of the muon anomalous magnetic moment, a_μ [1]. A persistent tension between theoretical predictions and the direct measurement of a_μ by the Muon $g-2$ experiment in Fermilab [2] motivates an independent, experimental measurement of the hadronic contribution. MUonE achieves this by studying the differential cross section of elastic muon-electron scattering using a high energy muon beam incident on low-Z targets [3].

The full MUonE concept consists of 40 identical tracking stations, each integrating a O(1 cm) thick scattering target and a series of silicon microstrip detectors, in order to precisely measure outgoing particle directions. In this way the effective target thickness is maximised and allows the collection of sufficient statistics in a reasonable running time.

Throughout June-August 2025 at the CERN SPS M2 beamline, a complete small-scale version of the experiment (known as Phase 1) [4], including three tracking stations, an electromagnetic calorimeter (ECAL), a muon filter, and a prototype beam momentum spectrometer (BMS) was operated to demonstrate the underlying technologies and validate the overall detector concept and performance requirements (figure 1). With all systems operating at the full 40 MHz sampling rate and a data acquisition system capable of performing online event selection on advanced FPGAs, Phase 1 recorded approximately 10 times the integrated luminosity (estimated $\sim 5\,\text{pb}^{-1}$ of elastic events) than the previous test run in 2023 [5]. With this dataset, the experiment aims to obtain confirmation of $\Delta\alpha_{\text{lep}}$ and a perform a measurement of $\Delta\alpha_{\text{had}}$ with O(20%) statistical accuracy. If successful, the Phase 1 run will serve as a major milestone toward the full experiment.

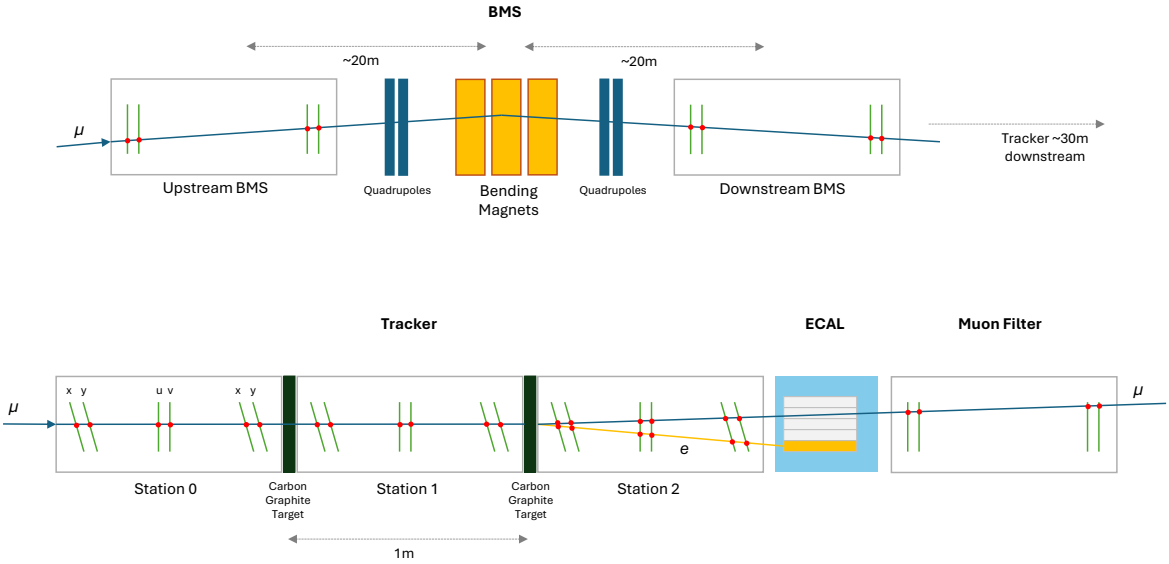

Figure 1. Overview of the MUonE Phase 1 detector at the SPS M2 beamline, including the beam momentum spectrometer (BMS) section (above), situated upstream of the three tracker stations, ECAL and the muon filter (below). Two 2 cm thick carbon graphite targets were installed in the tracker, generating the muon-electron scattering events required to extract a measurement of $\Delta\alpha_{had}$.

2 Detector & DAQ

2.1 2S modules

The Phase 1 demonstrator relies entirely on silicon modules known as 2S (2-strip sensor) modules, designed for the upgrade of the CMS Tracker for HL-LHC [6], whose characteristics and performance are essential for tracking under high-rate conditions. The M2 beamline delivers intensities of 1–2×10^8 muons at 160 GeV over a spill of approximately 5 s in duration. This demands a detector technology capable of sustaining a continuous sampling rate of around 40 MHz without dead time.

Each 2S module integrates two 10 cm × 10 cm, 320 µm-thick n-on-p sensors with 90 µm strip pitch, segmented into two approximately 5 cm long strips. The two sensors are separated by 1.8 mm but share the same read-out electronics allowing the possibility to detect correlated hit pairs using a programmable search window. These correlated hits form short track vectors known as "stubs". Not only are stub hits transmitted continuously at the 40 MHz sampling rate, but the correlation mechanism provides an effective tool for suppressing large-angle beam background as well as noise.

On the edges of the sensor the strips are read out by 16 CBC3.1 ASICs [7] which provide binary strip hit information and perform on-module stub finding. The two downstream CIC2.1 ASICs [8] aggregate data from 8 CBCs each, providing zero-suppression for full hit data and transmitting up to 16 stubs every eight 40 MHz cycles to the lpGBT serialiser chip [9], whereupon the data is sent on optical fibre to the DAQ at 5.12 Gb/s.

2.2 Tracker

The three Phase 1 stations contain six 2S modules each, grouped into three pairs with strips oriented orthogonally. The first and last pair of modules in a station both measure the (x,y) coordinates of passing particles, while the central pair of modules are rotated by 45° in order to provide a set of

2026 JINST 21 C04022

(u,v) coordinates to help resolve tracking ambiguities and permit robust pattern recognition. Modules measuring the (x,y) coordinates are intentionally tilted by ~ 233 mrad around the strip axis to increase charge sharing between adjacent strips [10], effectively reducing the pitch and improving spatial resolution to better than $\sim 15\,\mu$m.

The modules are mounted on precision Invar frames whose thermal expansion coefficient (~ 1.2 ppm/K) ensures stability at the $< 10\,\mu$m level. In the Phase 1 setup, both stations 1 and 2 include a 2 cm carbon graphite scattering target, while no target is installed in station 0 as it is intended to measure the incoming muon trajectory prior to scattering. Mechanical alignment is performed using a motorised system capable of micrometre positioning along and across the beam. During data taking, a holographic laser alignment scheme monitors long term stability.

2.3 Electromagnetic calorimeter (ECAL) & muon filter

The Phase 1 ECAL consists of a 5×5 matrix of $PbWO_4$ crystals repurposed from CMS [11], with a goal of measuring electrons with an energy resolution of $\sigma(E)/E \sim 1\%$ above 100 GeV and a position resolution of $\lesssim 1$ mm for the reconstructed electron impact point. Scintillation light from each crystal is read out by APDs, while front-end amplification is performed by the CMS MGPA chip [12]. Each channel is digitised on dedicated front-end boards using 14-bit ADCs at 40 MHz. Digital data from the ADCs are transferred via flex cables to an FC7 board [13] which serialises and transmits the data unsuppressed from all 25 channels at the full rate. The FC7 drives four optical links to the DAQ at 5.12 Gb/s, using the same lpGBT protocol as used by the 2S modules.

Meanwhile the muon filter is instrumented with an additional set of 2S tracking modules arranged as two (x,y) pairs on a mechanical structure similar to that used in a tracking station. As the resolution requirements for the muon filter are less demanding, the 2S modules are left un-tilted with respect to the beam axis. The muon filter enables identification of the scattered muon while electrons and other radiative background are absorbed in the ECAL.

Taken in combination, the ECAL and the muon filter are expected to provide the discrimination power needed to identify muon from electron tracks. This is especially important for scattering events in the kinematic region where the electron and muon scattering angles are very similar (< 5 mrad) and $\mu - e$ separation based solely on tracking becomes difficult.

2.4 Beam momentum spectrometer (BMS)

The BMS is essential to achieve the desired reduction in beam-related systematic uncertainties. Muons in the M2 line typically exhibit an energy spread of $\sigma(p)/p \sim 3.7\%$, but elastic scattering kinematics depends on the momentum of the incoming muon. The Phase 1 BMS uses two telescopes consisting of four 2S modules each. By positioning a telescope before and after the 16 Tm dipole magnets situated ~ 50 m upstream of the tracker stations, the measured deflection allows the per-muon momentum to be reconstructed. With each telescope providing an angular resolution of ~ 0.04 mrad, this should be sufficient to reduce the energy spread to below the 0.5% necessary for Phase 1. High precision mapping of the magnetic field in the region and a more complete alignment would allow the resolution on the incoming muons to be improved even further.

2026 JINST 21 C04022

2.5 Data acquisition & online selection

The MUonE DAQ operates triggerless, which means it must process every 40 MHz event from all subdetectors continuously. The DAQ is based on the Serenity platform [14], a high bandwidth ATCA processing card that provides up to 1.2 Tb/s of configurable optical IO, developed for use in the HL-LHC upgrade of CMS. The Phase 1 system utilises a Serenity Z prototype card that deploys two AMD-Xilinx KU15P FPGAs.

The DAQ receives 36 lpGBT links in total (5.12 Gb/s each) from all three tracking stations, calorimeter, muon filter and BMS. The firmware on the first FPGA decodes, aggregates, and analyses data from each of these input sources in real time. For example, stubs from the six modules in each of the tracking stations are extracted from the data stream, checked for errors, divided into individual events, and then reassembled into per-station fragments each corresponding to a single event. Every fragment is inspected at the full 40 MHz rate which allows the DAQ to identify events of interest.

The firmware on the second FPGA implements an AXI-Stream based event builder, collecting fragments from all subdetectors with consistent event IDs, and constructs Ethernet packets for data transmission from Serenity to commercial PCs. Up to eight 10 Gb/s UDP/IP ethernet links are implemented in the Phase 1 system, although in practice the acquisition rate following event selection is no more than 3 Gb/s on average ($\sim$ 10 Gb/s in-spill). Existing infrastructure provides for a dedicated 100 Gbps fibre-optic connection such that data can be transferred rapidly to EOS, a CERN-wide service for high capacity storage and low latency retrieval of physics data, for later offline processing. A Data Quality Monitoring instance running on the CERN OpenStack analyses a sample of events collected on EOS for rapid feedback on beam conditions and detector performance.

With an estimated aggregate raw data bandwidth of O(Tb/s) in the proposed full scale MUonE experiment, a real-time method of pre-selecting interesting events for later analysis is crucial to minimise eventual data storage and computing requirements. In Phase 1 an FPGA-based algorithm that applies topological criteria based on stub multiplicities is used to identify potential μ-e scatters. Simple occupancy-based logic is sufficient to suppress non-interacting muons while scattering events (with and without muon pile-up) are identified with $> 99\%$ efficiency. Random and pre-scaled passing muon triggers are also implemented to allow for regular calibration and alignment checks. Overall, this enables the event rate to be reduced from 40 MHz to an average rate of $\sim$ 500 kHz (1.5 MHz in-spill).

3 Commissioning the Phase 1 detector

Muon arrival times in the SPS M2 beamline are asynchronous with respect to the 40 MHz sampling clock used by all frontend ASICs. Additionally, with multiple detector elements distributed over $\sim$ 80 m, synchronisation and correlation of signals posed specific challenges. One advantage however of a DAQ with the ability to observe every 40 MHz sample at the back-end is that identifying the fixed delays between detectors becomes relatively trivial.

To align all the Phase 1 detectors in time following installation, a coarse synchronisation step using a reference 2S module provided alignment of the system to within 25 ns. Using a low-intensity muon beam, this step required identifying the clock cycle where the highest correlation of stubs with the reference module is observed for each of the modules in the tracker, muon filter and BMS. Since every clock cycle can be captured, this procedure rapidly yields a set of delay settings to be applied to each module (figure 2).

2026 JINST 21 C04022

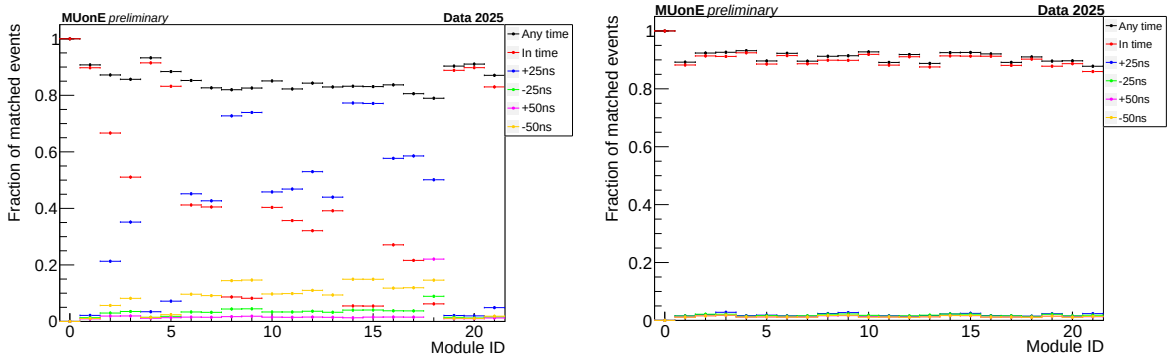

Figure 2. Ratio of events with a stub in a given module when a single stub is recorded in the reference module (station 0, module 0) for the 18 tracker and 4 muon filter 2S modules, before any synchronisation in time (left), and following both coarse and fine synchronisation steps (right). The different series of points represent the ratio of events where the stubs in the given module are found in the same clock cycle (in time), or in previous/subsequent clock cycles (+/- 25/50 ns) as the stub in the reference module. During coarse synchronisation the appropriate coarse delay settings can be extracted from the clock cycle that maximises the ratio for each individual module.

Once these delays were configured, a fine synchronisation procedure was performed at the module level. Each CBC includes an on-chip Delay Locked Loop (DLL) capable of introducing phase shifts in 1 ns increments across the 25 ns clock window. As illustrated in figure 3, by scanning all DLL phases

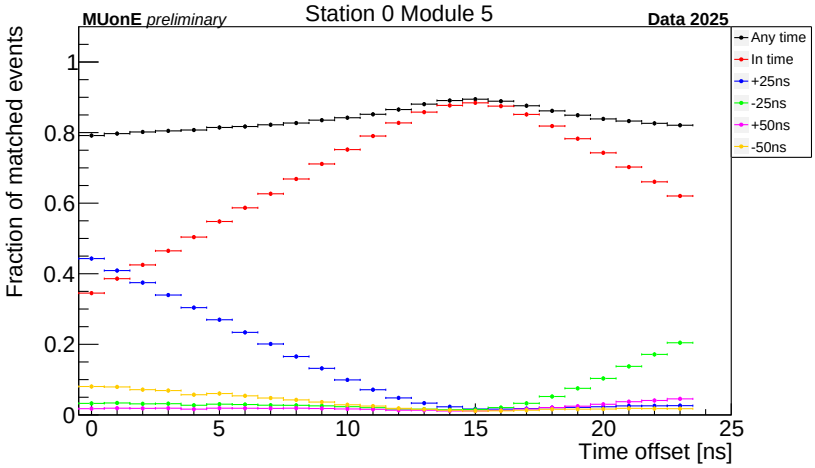

Figure 3. Example of a fine synchronisation scan (here for station 0, module 5) showing the ratio of events with a stub in a given module when a single stub is recorded in the reference module (station 0, module 0), measured as a function of the phase offset (DLL setting). The different series of points represent the ratio of events where the stubs in the scanned module are found in the same clock cycle (in time), or in previous/subsequent clock cycles (+/- 25/50 ns) as the stub in the reference module. In each case, the module under study is eventually configured with a DLL setting that maximises the in time ratio (here 15 ns).

and measuring the coincidence rate with the reference module, the peak of the correlation distribution was identified and used to set the optimal sampling phase. This process was repeated for every 2S module across all stations, the muon filter, and the BMS resulting in global sub-ns timing uniformity.

2026 JINST 21 C04022

The ECAL was synchronised to the tracker using a dedicated 40 GeV electron run at low intensity. Since the shaped pulse at the output of the MGPA has a rise time of around 50 ns, ECAL signals span multiple clock cycles. By comparing the maxima of the pulse shapes in the ECAL with the presence of stubs in the tracker, the relative delay between the two systems could be identified and configured in the DAQ. Only a coarse synchronisation is required in this case as the DAQ records up to 15 consecutive samples of non-zero-suppressed ECAL data for every selected event.

In addition to system synchronisation, other detector commissioning steps included tuning of the 2S module response to maximise performance. As described in [15], bias-voltage scans confirmed full sensor depletion above ~ 300 V. All modules were biased at 400 V for the duration of the run, except for two modules which exhibited significantly higher leakage current and were conservatively kept at 350 V. Scans were also performed on all modules to tune the CBC discriminator thresholds to maximise efficiency and minimise noise occupancy. A threshold of ~ 7500 electrons was determined to be an optimal working point for all modules, corresponding to approximately 9 times the average per-strip noise.

4 Preliminary performance results

During the 3-month Phase 1 run in 2025, over 5×10^{11} selected events were recorded in total, amounting to around 500 TB of data stored on EOS. While a detailed analysis towards the physics goals of the Phase 1 run is ongoing, some preliminary results on detector performance are highlighted here.

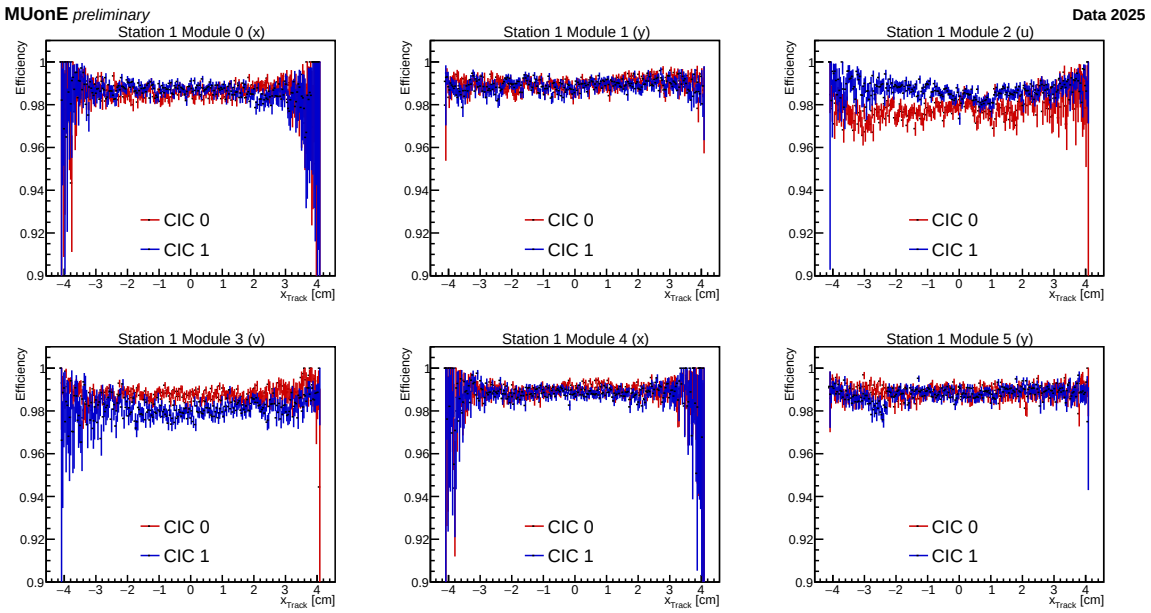

Figure 4. Stub efficiency for the 2S modules in the second station as a function of the track position when extrapolated to the surface of the module under study. The two colours represent the two CICs on a 2S module.

Figure 4 shows the stub efficiency for the 2S modules in the second station as an example of the performance of the tracking systems. Efficiency is estimated by preselecting events with one stub in every other tracker module than the module under study, which are then used to reconstruct a track. Only good quality tracks (Prob(χ^2/ndof) >1%) are used, and fiducial cuts are applied to eliminate

2026 JINST 21 C04022

border effects at module edges for example. Any stub found to within 200 µm of the position estimated by extrapolating the track to the surface of the module under study counts towards the efficiency. Each module half, corresponding to readout via either CIC (CIC0 or, CIC1), is treated independently and efficiency is plotted as a function of extrapolated position along the local coordinate representing strip number. The efficiency for most 2S modules during the Phase 1 run was measured to be between 98–99% which is consistent with operation of 2S modules in an asynchronous beam.

By applying a preselection on events with a single stub in each module of the tracker and again reconstructing tracks using stubs from every module except for one under study, it is possible to measure the unbiased residuals — providing an estimate of detector resolution. The unbiased residuals are defined as the difference between the position of the stub on the module under study and the track position extrapolated to the surface of the same module. Figure 5 shows the unbiased residuals for each of the 2S modules in the second station.

The residuals for tilted modules are clearly smaller (15 µm) than for non-tilted modules (23 µm) as expected. It should be noted that the standard deviation of the unbiased residuals is not same as the intrinsic resolution of the module which requires that the error on the track fit to be subtracted from the residual. This is currently work in progress.

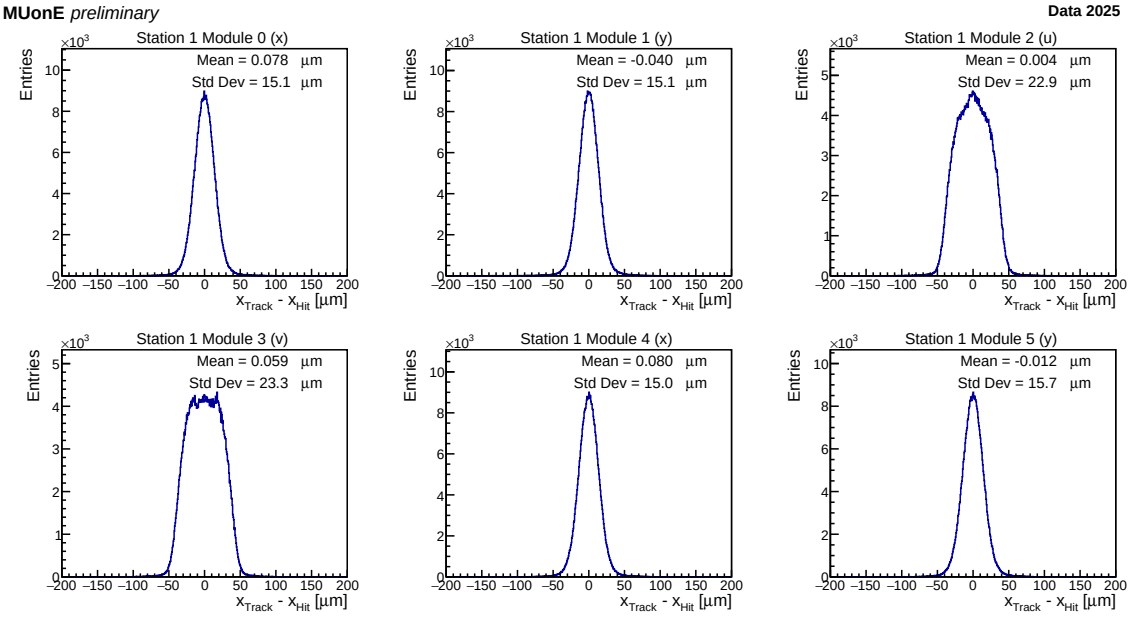

Figure 5. Unbiased residuals for the modules in the second tracking station. The residuals for tilted modules are smaller than for non-tilted modules due to the increased charge sharing and smaller effective pitch.

Preliminary elastic scattering curves showing the correlation between outgoing μ-e track angles have been extracted from a small subset of the data collected in 2025. By reconstructing tracks in all three stations, and applying a loose elastic selection criteria, figure 6 (left) shows the 2D distribution of scattering angles for the two outgoing tracks. The particle identity is ambiguous at angles below 5 mrad (indicated by the region above the green dashed line) and therefore tracks are labelled according to the maximum and minimum angle, respectively plotted on the x and y axis. Figure 6 (right) shows that by extrapolating tracks to the muon filter and tagging tracks as muons if they successfully match with hits in the muon filter system, it is possible to correctly identify muon tracks vs. electron tracks and therefore reconstruct the elastic scattering curve below the 5 mrad limit.

2026 JINST 21 C04022

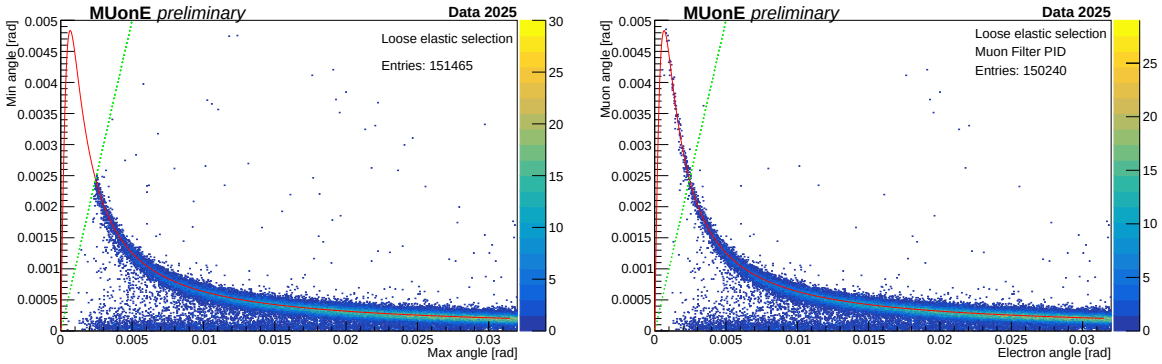

Figure 6. 2D distribution of the scattering angles of the two outgoing tracks reconstructed in events passing a loose elastic selection based only on tracker measurements (left) and including particle identification using the muon filter (right). The green dashed line corresponds to equal scattering angles. The red curve shows the kinematic correlation between muon and electron scattering angles expected for elastic scattering with a beam energy of 160 GeV.

5 Conclusions

The MUonE Phase 1 run has concluded successfully, with all detector subsystems operating stably at the full 40 MHz rate and delivering good performance over the duration of the data-taking period. Synchronisation was demonstrated across the tracker, ECAL, muon filter, and BMS, while preliminary studies confirm stub efficiencies > 98%, excellent spatial resolution, and the capability to reconstruct elastic μ-e scattering events. With over 5×10^{11} selected events recorded, detailed analyses aimed at achieving the Phase 1 physics objectives are currently underway. The results so far provide encouragement towards validation of the underlying detector concept and offer a solid foundation for the design of the full MUonE experiment.

Acknowledgments

The MUonE collaboration gratefully acknowledges the support and contributions of the CMS Tracker group including the provision of 2S modules and readout infrastructure to produce the results shown in these proceedings.

References

[1] MUonE collaboration, *Letter of Intent: the MUonE project*, CERN-SPSC-2019-026 (2019).

[2] Muon $g-2$ collaboration, *Measurement of the Positive Muon Anomalous Magnetic Moment to 127 ppb*, *Phys. Rev. Lett.* **135** (2025) 101802 [arXiv:2506.03069].

[3] MUonE collaboration, *Measuring the leading hadronic contribution to the muon g-2 via μe scattering*, *Eur. Phys. J. C* **77** (2017) 139 [arXiv:1609.08987].

[4] MUonE collaboration, *Proposal for phase 1 of the MUonE experiment*, CERN-SPSC-2024-015 (2024).

[5] MUonE collaboration, *The MUonE experiment: a novel way to measure the hadronic contribution to the muon g-2*, *PoS* **ICHEP2024** (2025) 345.

[6] CMS collaboration, *The Phase-2 Upgrade of the CMS Tracker*, CERN-LHCC-2017-009 (2017).

2026 JINST 21 C04022

[7] K. Uchida et al., *Results from the CBC3 readout ASIC for CMS 2S-modules*, *Nucl. Instrum. Meth. A* **924** (2019) 175.

[8] S. Viret et al., *CIC2: a radiation tolerant 65 nm data aggregation ASIC for the future CMS tracker*, 2022 *JINST* **17** C05016.

[9] P. Moreira et al., *lpGBT: Low-Power Radiation-Hard Multipurpose High-Speed Transceiver ASIC for High-Energy Physics Experiments*, *IEEE Trans. Nucl. Sci.* **72** (2025) 24.

[10] Tracker Group of the CMS collaboration, *Beam test performance studies of CMS Phase-2 Outer Tracker module prototypes*, 2024 *JINST* **19** P10032 [arXiv:2404.08794].

[11] CMS collaboration, *The CMS Experiment at the CERN LHC*, 2008 *JINST* **3** S08004.

[12] M. Raymond, G. Hall, J. Crooks and M. French, *The MGPA electromagnetic calorimeter readout chip for CMS*, *IEEE Trans. Nucl. Sci.* **52** (2005) 756.

[13] M. Pesaresi et al., *The FC7 AMC for generic DAQ & control applications in CMS*, 2015 *JINST* **10** C03036.

[14] T. Mehner et al., *Lessons learned while developing the Serenity-S1 ATCA card*, 2024 *JINST* **19** C02018 [arXiv:2311.02222].

[15] D. Monk, *40 MHz readout of CMS silicon modules in a high intensity beam*, *Nucl. Instrum. Meth. A* **1068** (2024) 169783.

2026 JINST 21 C04022